

Electrostatic induction of the electric field into free-flow electrophoresis devices

Dirk Janasek,* Michael Schilling, Andreas Manz and Joachim Franzke

Received 23rd February 2006, Accepted 8th May 2006

First published as an Advance Article on the web 15th May 2006

DOI: 10.1039/b602815b

The electrostatic induction of an applied voltage causes electrophoretic separation under free-flow conditions and no electrolysis or electric current flowing between the metal electrodes was observed.

The field of miniaturised total analysis systems (μ TAS) or 'Lab-on-a-Chip' has grown tremendously, and many miniaturised approaches of known conventional analytical techniques have been introduced, e.g. capillary electrophoresis, chromatography and PCR.¹ Among the separation techniques, capillary electrophoresis (CE) is the most employed because of its simplicity in fabrication, setup and use.

There are some drawbacks for CE for on-line monitoring purposes, since it is a discontinuous technique alternating between injection and separation. Secondly, the small volume of sample which is injected in order to obtain a good separation makes it difficult to employ CE in preparative scale. Therefore, free-flow electrophoresis (FFE) was developed. In contradiction to CE where the electric field is applied along the capillary and thus a longitudinal separation is obtained, in FFE the electric field is applied perpendicular to a hydrodynamic flow through the separation chamber. Consequently, each molecule is affected by two perpendicular vectors causing a movement at an angle to the flow and thus resulting in a geometrically speaking two-dimensional separation.

Besides commercially available bench-top FFE devices with separation bed volumes in the range of tens of millilitres² there are also miniaturised devices with bed volumes of microlitres and sub-microlitres reported for zone electrophoretic mode,^{3–6} isoelectric focussing mode^{7,8} and isotachophoretic mode.⁹ Obeying the scaling laws,¹⁰ they could be employed for preparative purposes of small sample volumes as well as for analytical applications because of their fast performance.

The greatest challenge in the fabrication of μ -FFE devices is the method of voltage transfer to form the electric field in the separation chamber. Macounová *et al.* reported a device where the electrodes were in direct contact with the liquid.¹¹ Having direct contact between a metal electrode and an aqueous solution means that electrolysis occurs resulting in gas bubble formation at higher potentials. In that publication, palladium electrodes were used because Pd is able to recombine O₂ and H₂ to H₂O avoiding gas bubble formation. The authors showed separations with applied voltages as high as 2.2 V resulting in an electric field of 1.73 V cm⁻¹. Even with this "non-gassing" property of Pd, higher

voltages would not be applicable because of the limited capacity of Pd for gas adsorption and recombination.

In conventional bench-top FFE instruments electrodes are separated from the separation department by a membrane serving as an electrolyte bridge. In microfabrication, the incorporation of such a membrane is difficult. Zhang and Manz described a μ -FFE device where 108 fine channels connected the separation chamber and the remote electrode reservoir on each side serving as an electrolyte bridge.⁵ Like a membrane, these fine channels allowed electric conduction while at the same time reduced pressure flow between the electrode reservoirs and the separation chamber. The disadvantage of this layout was the small total cross-section of the connection channels causing a high ohmic resistance and thus a high voltage drop in the channels. Only 4.45% of the totally applied voltage reach the separation chamber generating the electric field across the compartment.

Fonslow and Bowser have reported a μ -FFE device with 50% of the totally applied voltage generating the electric field by using a bigger value of the total cross-section of the connecting channels.⁶ In order to prevent liquid leakage from the electrode channel to the separation channel and *vice versa*, the hydrodynamic flow in the electrode channel had to be adapted to the flow in the separation compartment. Meeting that balanced condition seems difficult; in the results described in that article that state was not met.

Another approach was reported by Albrecht *et al.*⁸ They used packed polymer beads to isolate the separation compartment from the metal electrode surface and could obtain a voltage drop across the separation channel of 21 to 66% of the applied voltage.

Kohlheyer *et al.* integrated photo-polymerised, ion permeable membranes to hydrodynamically isolate the separation compartment from the side electrodes.¹² With such a device they achieved a very efficient use of the applied voltage and established a wide pH gradient from pH 3 to 10 in isoelectric focussing experiments. However, the device is more laborious to fabricate than the above mentioned approaches.

In this communication we describe a μ -FFE device where the electric field is generated by electrostatic induction across an insulating wall. Electrostatic induction is based on the displacement of charges across an insulator by dipole orientation (Fig. 1) which has also been employed for dielectric barrier discharges¹³ and "FlowFETs".¹⁴ Presuming the surface of an electrode is positively charged, then dipoles inside an adjoining insulating material orient in such a way that the negative sides are facing the positive surface of the anode. Like a chain, the dipoles transfer the charges from the surface of the electrode to the distant surface of the insulator. Thus, the insulator-liquid interface has the same

ISAS—Institute for Analytical Sciences, Bunsen-Kirchhoff-Str. 11, D-44139, Dortmund, Germany. E-mail: d.janasek@ansci.de; Fax: +49 (0)231 1392-120; Tel: +49 (0)231 1392-202

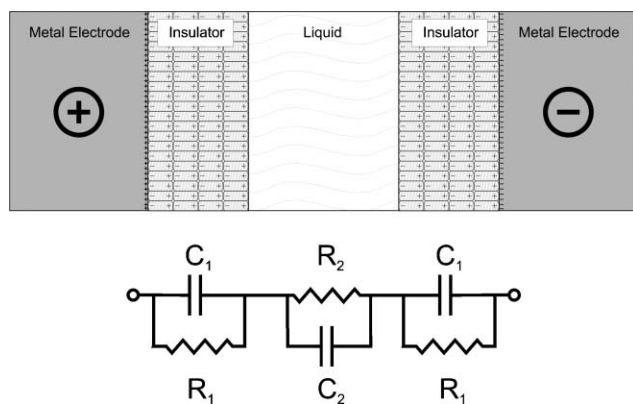


Fig. 1 Principle of electrostatic induction by charge displacement caused by dipole orientation. Lower panel: Equivalent circuit diagram. The capacitor C1 and the resistor R1 for the dielectric barrier are in the range of pF and TΩ, respectively; C2 and R2 for the liquid compartment are in the range of tens of fF and a few Ω, respectively.

polarity as the metal electrode. The amount of charges Q depends on the specific characteristic of the insulator, ϵ_r :

$$Q = UC \quad \text{and} \quad (1)$$

$$C = \epsilon_0 \epsilon_r \frac{A}{d}, \quad (2)$$

where U is the voltage applied, C the capacity of the barrier, ϵ_0 and ϵ_r the absolute and relative permittivity, respectively, and A is the area and d the distance of the barrier. Typical values for ϵ_r are 5–16 for glass and 100–10 000 for ceramics, respectively.

The displaced charges at the anodic and cathodic side of the separation compartment generate the electric field which causes electrophoresis. Although the polarity of the other side of the insulator is the same as the metal electrode, no current flows resulting in no electrolysis.

In order to show the generation of an electric field, focussing of fluorescein should be performed in isotachophoretic mode as shown in ref. 9. Isotachopheresis (ITP) is carried out in a two-buffer system, where the ion mobilities in the leading and terminating electrolyte are higher or lower than the mobilities of all the analyte ions, respectively, generating a gradient in the electric field. This gradient causes a separation, stacking in consecutive zones, and a focussing of the analyte sample according to Kohlrausch's regulating function.¹⁵

The chip was fabricated in glass by photolithography and wet-etching. The layout of the chip is depicted in Fig. 2. The separation chamber was designed similarly to the one described previously.⁹ The separation compartment (12.2 mm long, 4.4 mm wide) contained 31 104 diamond-shaped posts of 40 μm edge length. The distance between the centre points of two adjacent posts was 50 μm resulting in the formation of 10 μm channels between the posts. Sample solution and collateral buffer were introduced into the separation chamber *via* 64 inlet channels in such a way that the sample solution was bordered by terminating and leading electrolyte, respectively, meeting the ITP demands. The solution left through 64 outlet channels. The depth of the structures was wet-etched to 30 μm.

In the same process of etching the structures for the fluid handling, at each side of the separation chamber grooves were

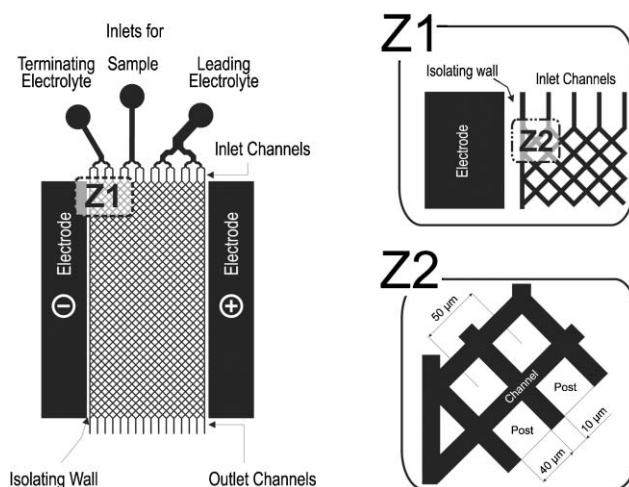


Fig. 2 Layout of the chip.

fabricated which finally contained the electrodes. A 146 μm glass wall between these grooves and the separation compartment served as the dielectric barrier (Fig. 3).

After bonding, Wood's alloy was filled into the electrode groove-channels and contacted with tungsten wires. At the inlet and outlet access holes for electrolyte and sample, interface connectors were manufactured.

For experiments, the chip was placed on the stage of an inverted confocal microscope (Leika, Milton Keynes, UK) equipped with a 50 W mercury lamp for fluorescence imaging. The fluorescence emission was recorded by a colour CCD camera (Sony, Japan). The electrodes were connected to a high power supply (F.u.G. Elektronik GmbH, Rosenheim, Germany). The power supply was also connected to a multimeter (Precision Gold M215, RS Components Ltd., UK) for current monitoring. The multimeter could measure currents down to 100 nA.

The hydrodynamic flow through the separation chamber was generated by pumping of the leading and terminating electrolytes and the sample solution by means of three syringe pumps (Technical & Scientific Equipment GmbH Bad Homburg, Germany) in the velocity ratio of 2 : 1 : 1, respectively. The interface connectors for electrolyte and sample solutions were connected to the syringe pumps *via* silicon tubes.

For the ITP experiments, leading and terminating buffer consist of 10 mM chloride adjusted to pH 9.3 using ethanolamine and 6 mM β-alanine adjusted to pH 10.2 with barium hydroxide, respectively.

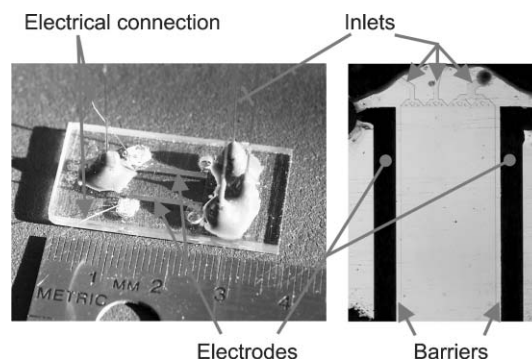


Fig. 3 Photograph and transmission micrograph of the chip.

De-ionised water was used in all experiments. The chemicals were of analytical grade. Fluorescein sodium salt and ethanolamine were purchased from Sigma-Aldrich-Fluka (Taufkirchen, Germany). β -Alanine, hydrochloric acid, methylhydroxyethyl cellulose (MHEC) and barium hydroxide were obtained from Merck Darmstadt, Germany. Wood's alloy was purchased from Goodfellow (Cambridge, UK).

For the experiments, high voltage and UV radiation were applied. High power and UV radiation pose danger for health and thus demand special caution.

As seen in eqn (1) and (2), the amount of transferred charge Q depends on the material of the insulator indicated by ϵ_r , on the area A and the distance of the insulating barrier d . For given material and area determined by the geometry of the separation compartment, a thinner barrier causes better, more efficient transfer of charge Q . On the other hand, the dielectric strength has to be taken in consideration which is 100–400 kV cm⁻¹ for glass. This characteristic favours thicker barriers. In order to obtain a high ratio of voltage available across the separation chamber to applied voltage, a thickness of the dielectric barriers of 146 μ m was fabricated, which determines a capacity of 0.1 pF for one barrier and a breakthrough voltage of approximately 3.6 kV.

Fig. 4A shows the fluorescence micrograph obtained when a hydrodynamic flow of sample and buffer solutions was generated by pumping but no voltage was applied. It is clearly seen that the fluorescein sample was just flowing through the chamber without any change indicated by the homogenous colour of the stream. The slight bending towards the cathode was caused by the non-synchronised pulsation of the individual syringe pumps. When a voltage of 150 V was applied to the electrodes, an isotachophoretic focussing of the sample stream between the leading and the terminating electrolyte occurred a few micrometres after the inlet (Fig. 4B). As seen in the change of colour, the intensity of fluorescence increased corresponding to the increase of concentration.

The successful performance of the isotachophoretic focussing has given evidence of the existence of an electric field in the separation chamber. At the same time, no electric current could be measured between the electrodes using the multimeter.

In order to explain this phenomenon, a second experiment was carried out where the solutions were not flowing. When a voltage was applied no electrophoresis occurred. We presume that under these conditions charges were on the surface of the insulator, however opposite charges moved to that surface and neutralised

those charges resulting in no potential difference and no electric field anymore. However, under flowing conditions the neutralising charges were continuously moved out of the separation compartment. Under these circumstances an electric field can be generated resulting in electrophoresis.

Using eqn (1) and (2), it could be calculated that 50% of the total applied voltage was generating the electric field in the separation chamber. This corresponds to 180 V cm⁻¹, which is in the range of electric fields used in previous experiments.⁹

In another experiment an identical device was used and even higher voltages than the breakthrough voltage were applied. During this time, the thin dielectric barriers were damaged. The generation of tiny gas bubbles at the anodic side of the chamber could be observed even when the voltage was decreased back to 150 V. The volume increase of such a gas bubble was approx. 0.6 nl s⁻¹. The gas formation indicated electrolysis caused by the current flowing through a tiny crack in the dielectric barrier provoked by voltages higher than the breakthrough voltage. When electrolysis was observed, no isotachophoretic focussing could be observed any longer since the charge displacement across the dielectric barrier was disturbed.

A new approach for inducing the electric field into free-flow electrophoresis devices was successfully demonstrated. Electrostatic induction overcomes some major drawbacks of miniaturised FFE devices presented recently, which are electrolysis or low voltage transfer efficiency, and on the other hand leakage or a difficult fabrication process. The insulating barriers employed here can be fabricated in the same process as the whole microfluidic structure. The 50% efficiency of total applied voltage transferred into the separation chamber can be further improved by fabrication of smaller barriers and the use of chip material with a higher relative permittivity. However, it has to be noted that the described approach works only in flowing systems. In order to understand the phenomenon in more detail, additional experiments have to be carried out.

Acknowledgements

The authors thank Mr Ulrich Marggraf for his help during the micromachining process, Prof. Andreas Neyer from University of Dortmund for providing cleanroom access in his department, and Mr Richard Heming for helpful discussions. The financial support by the Ministerium für Innovation, Wissenschaft, Forschung und Technologie des Landes Nordrhein-Westfalen, by the Bundesministerium für Bildung und Forschung, and by the European Community (CellPROM project, contract no. NMP4-CT-2004-500039 under the 6th Framework Programme for Research and Technological Development) is gratefully acknowledged.

Notes and references

- 1 D. Reyes, D. Iossifidis, P.-A. Auroux and A. Manz, *Anal. Chem.*, 2002, **74**, 2623–2636; P.-A. Auroux, D. Iossifidis, D. Reyes and A. Manz, *Anal. Chem.*, 2002, **74**, 2637–2652; T. Vilkner, D. Janasek and A. Manz, *Anal. Chem.*, 2004, **76**, 3373–3386.
- 2 H. Canut, J. Bauer and G. J. Weber, *J. Chromatogr., B*, 1999, **722**, 121–139.
- 3 D. E. Raymond, A. Manz and H. M. Widmer, *Anal. Chem.*, 1994, **66**, 2858–2864; D. E. Raymond, A. Manz and H. M. Widmer, *Anal. Chem.*, 1996, **68**, 2515–2522.

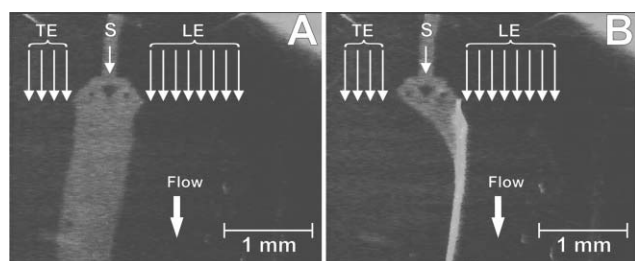


Fig. 4 Isotachophoretic behaviour of a fluorescein sample if (A) no voltage and (B) 150 V, respectively, were applied. Total flow rate $v = 20 \mu\text{l min}^{-1}$; $c_{\text{Fluorescein}} = 20 \mu\text{M}$. Abbreviations: TE—terminating electrolyte, S—sample, LE—leading electrolyte. Picture: dark gray—no fluorescence, light gray—highest fluorescence

- 4 A. Chartogne, U. R. Tjaden and J. van der Greef, *Rapid Commun. Mass Spectrom.*, 2000, **14**, 1269–1274; H. Kobayashi, K. Shimamura, T. Akaida, K. Sakano, N. Tajima, J. Funazaki, H. Suzuki and E. J. Shinohara, *J. Chromatogr., A*, 2003, **990**, 169–178.
- 5 C.-X. Zhang and A. Manz, *Anal. Chem.*, 2003, **75**, 5759–5766.
- 6 B. R. Fonslow and M. T. Bowser, *Anal. Chem.*, 2005, **77**, 5706–5710.
- 7 Y. Xu, C.-X. Zhang, D. Janasek and A. Manz, *Lab Chip*, 2003, **3**, 231–234.
- 8 J. Albrecht, S. Gaudet and K. F. Jensen, in *9th International Conference on Miniaturized Systems for Chemistry and Life Sciences*, Boston, MA, USA, 2005, vol. 2., pp. 1537–1539.
- 9 D. Janasek, M. Schilling, J. Franzke and A. Manz, *Anal. Chem.*, 2006, DOI: 10.1021/ac060063l.
- 10 A. Manz and J. C. Eijkel, *Pure Appl. Chem.*, 2001, **73**, 1555–1561.
- 11 K. Macounová, C. R. Cabrera and P. Yager, *Anal. Chem.*, 2001, **73**, 1627–1633.
- 12 D. Kohlheyer, G. A. Besselink, S. Schlautmann and R. B. Schasfoort, *Lab Chip*, 2006, **6**, 374–380.
- 13 M. Miclea, K. Kunze, G. Musa, J. Franzke and K. Niemax, *Spectrochim. Acta, Part B*, 2001, **56**, 37–43.
- 14 R. B. Schasfoort, S. Schlautmann, J. Hendrikse and A. van den Berg, *Science*, 1999, **286**, 942–945.
- 15 F. W. Kohlrausch, *Ann. Phys. Chem.*, 1897, **62**, 209–239.

Find a SOLUTION

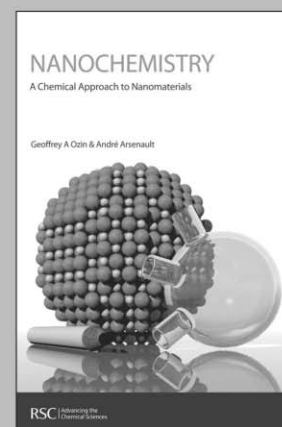
... with books from the RSC

Choose from exciting textbooks, research level books or reference books in a wide range of subject areas, including:

- Biological science
- Food and nutrition
- Materials and nanoscience
- Analytical and environmental sciences
- Organic, inorganic and physical chemistry

Look out for 3 new series coming soon ...

- RSC Nanoscience & Nanotechnology Series
- Issues in Toxicology
- RSC Biomolecular Sciences Series



RSCPublishing

www.rsc.org/books

28040542